

# Analysis of Generalized Selection Diversity Systems in Wireless Channels

A. Annamalai, *Member, IEEE*, Gautam Deora, and C. Tellambura, *Senior Member, IEEE*

**Abstract**—Motivated by practical considerations in the design of low-complexity receiver structures for wideband cellular code division multiple access, millimeter wave, and ultrawideband communications, the study on the generalized selection combining (GSC) receiver that adaptively combines a subset of  $M$  “strongest” paths out of  $L$  available paths has intensified over the past few years. This paper derives concise analytical expressions for the moment generating function (MGF) of the  $GSC(M, L)$  output signal-to-noise ratio when the fading statistics are independent and identically distributed. The novelty of this mathematical framework in computing the MGF relies on the fact that it allows all common multipath fading channel models (Rayleigh, Rician, Nakagami- $m$ , and Nakagami- $q$ ) to be treated in a unified sense. It also leads to a much more computationally efficient formula than those available in the literature and is valid for any combinations of  $M$  and  $L$  values. Using these newly derived MGFs, a unified error probability analysis for many coherent and noncoherent digital-modulation/detection schemes in a myriad of fading environments was provided.

**Index Terms**—Coherent receiver, digital communications, diversity methods, quadratic receiver, reduced complexity receiver structures.

## I. INTRODUCTION

THE generalized selection combining (GSC) scheme aims to mitigate the detrimental effects of deep fades experienced in wireless channels by applying an optimal linear combining rule to a subset of the “strongest” available diversity paths, thereby reducing the receiver complexity and cost (i.e., fewer electronics and lower power consumption). If the branches are coherently combined before signal detection, then we refer the diversity combining scheme as coherent GSC [1]. In noncoherent GSC [2], noncoherent combining of diversity branches is implemented after signal detection.

The GSC receiver merits consideration in a numerous practical applications. For example, in wideband code division multiple access (CDMA) and ultrawideband communications, the number of available correlators will limit the number of multipaths that can be utilized in a typical rake combiner. It also

Manuscript received August 26, 2002; revised February 23, 2003 and March 28, 2003. The review of this paper was coordinated by Dr. M. Stojanovic.

A. Annamalai is with the Bradley Department of Electrical and Computer Engineering, Virginia Tech. Advanced Research Institute, Arlington, VA 22203 USA (e-mail: annamalai@vt.edu).

G. Deora was with the Bradley Department of Electrical and Computer Engineering, Virginia Tech., Blacksburg, VA 220012 USA. He is now with the Applied Technology Group, Tata Infotech, Mumbai, India (e-mail: gdeora@vt.edu).

C. Tellambura is with the Department of Electrical and Computer Engineering, University of Alberta, Edmonton, AB T6G 2V4, Canada (e-mail: chintha@ece.ualberta.ca).

Color versions of Figs. 2–9 are available online at <http://ieeexplore.ieee.org>. Digital Object Identifier 10.1109/TVT.2006.878564

reduces the complexity of implementation for antenna arrays in millimeter-wave communications and improves the throughput performance of packet radio networks employing “selective packet combining.” Performance analyses of the coherent and noncoherent GSC receivers are also important from a theoretical viewpoint because  $GSC(1, L)$  and  $GSC(L, L)$  are simply the classical selection combining and maximal-ratio combining (coherent detection) or postdetection equal-gain combining (noncoherent detection) receiver, respectively.

Previous studies on GSC have been limited to only the Rayleigh [1]–[9] and Nakagami- $m$  channels [10]–[15]. While a Rayleigh model may be appropriate for macrocells, it is customary to model the fading signal amplitudes in microcellular and picocellular environments such as Rician distributed since the propagation paths usually consist of one strong direct line-of-sight component and many random weaker components. The appropriateness of this model has been validated by numerous field measurements. Moreover, Stein [17] and several other researchers have shown that the Nakagami- $m$  approximation for a Rician random variable (RV) suggested by Nakagami [18] tends to overestimate the receiver performance, particularly at large SNRs, owing to the fact that the tails of the Rician and its Nakagami- $m$  approximation<sup>1</sup> distributions do not fit very closely.

Despite the above reasons, performance analyses of both the coherent and noncoherent  $GSC(M, L)$  receivers in Rician multipath fading channels are not available in the literature. The primary difficulty stems from the fact that the ordered SNRs  $\gamma_{(k)}$  [obtained after rearranging the SNRs of all the  $L$  diversity branches  $\gamma_1, \gamma_2, \dots, \gamma_L$  in descending order, such that  $\gamma_{(1)} \geq \gamma_{(2)} \geq \dots \geq \gamma_{(L)}$ ], because of the inequalities among them, are necessarily dependent. Consequently, finding the moment generating function (MGF) of a linear sum of ordered RVs  $\gamma_{gsc} = \sum_{k=1}^M \gamma_{(k)}$  (i.e., GSC output SNR) is generally much more difficult than for the unordered RVs.

In the past, numerous attempts have been made to compute the MGF of ordered exponential [1]–[3] and gamma variates [12]–[15], resulting in various complicated formulas. Nevertheless, a few of them also treat the nonidentical fading case (e.g., [3] and [14]). Furthermore, the existing mathematical approaches do not lend themselves to the performance

<sup>1</sup>It is noted that the real importance of the Nakagami- $m$  fading model lies in the fact that it offers features of analytical convenience in comparison to the Rician distribution. However, the goodness-of-fit tests used by ionospheric physicists to match measured scintillation data to a Nakagami- $m$  distribution do not give a special weighting to the deep-fading tail of the distribution [17]. As a result, we sometimes have a better fit near the median of the distribution than in the tail region, although the tail behavior is of greater significance to communication systems performance analysis.

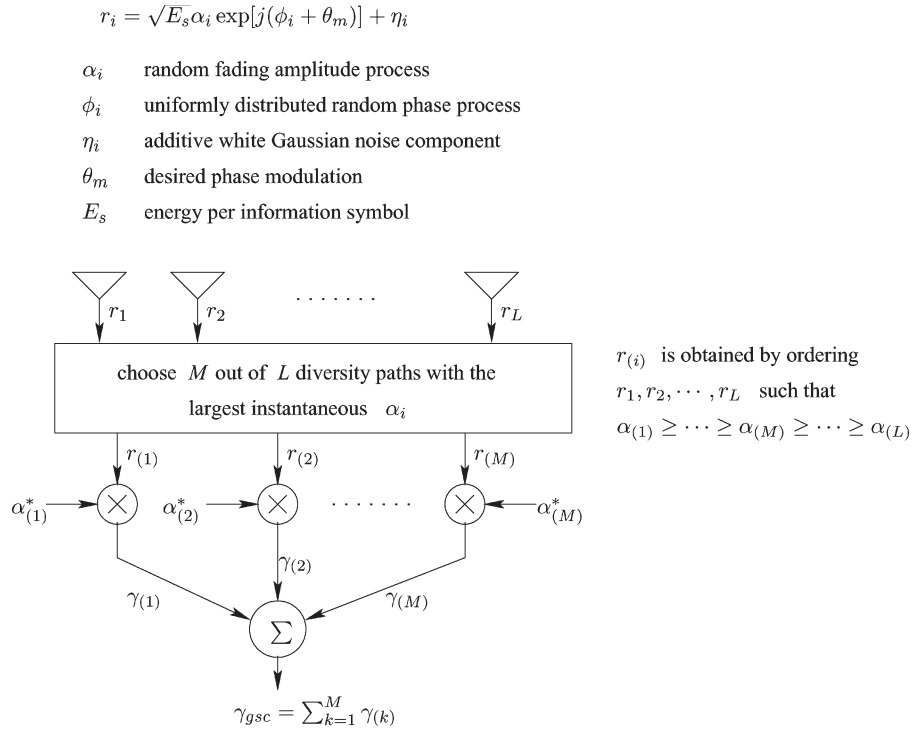


Fig. 1. Block diagram of a GSC( $M, L$ ) diversity receiver.

evaluation of GSC receivers in Rician channels easily. This paper develops a new mathematical framework for analyzing the GSC receiver performance with independent and identically distributed (i.i.d.) fading statistics in a variety of fading environments, including the Rician fading channel model.

One of the attractive features of our approach is that the MGF of GSC( $M, L$ ) output SNR for all common fading channel models as well as for all combinations of  $M$  and  $L$  values can be simply expressed in terms of only a single integral (with finite integration limits) whose integrand is composed of tabulated functions. For the special cases of Rayleigh and Nakagami- $m$  channel models, this integral may be further simplified into a closed-form formula. By utilizing these MGFs, we then compute several important performance metrics of the coherent and noncoherent GSC receiver structures, including the average bit or symbol error probability of different binary and  $M$ -ary modulation schemes, outage rate of error probability, and mean combined SNR at the GSC receiver output.

The remainder of this paper is organized as follows. Section II derives the MGF, probability density function (PDF), and cumulative distribution function (CDF) of  $\gamma_{gsc}$ , with the assumption of i.i.d. fading statistics. Several closed-form formulas for the MGF of  $\gamma_{gsc}$  in Rayleigh and Nakagami- $m$  fading channels are derived in Appendix B. In Section III, we utilize the MGF to unify the error probability analysis for a wide range of digital-modulation schemes in conjunction with the coherent and noncoherent (quadratic) GSC( $M, L$ ) receivers. Finally, the major results are summarized in Section IV.

## II. GSC( $M, L$ ) COMBINER OUTPUT STATISTICS

In this section, we will derive analytical expressions for the GSC( $M, L$ ) combiner output statistics by modeling the

branch amplitudes as i.i.d. Rayleigh, Rician, Nakagami- $m$ , or Nakagami- $q$  RVs. These expressions can be applied directly in computing the average bit error rate (ABER) or the average symbol error rate (ASER) and outage probability for different modulation schemes.

### A. MGF of GSC Output SNR

From [19], we know that when  $M$  strongest diversity branches are selected from a total of  $L$  available i.i.d. diversity branches, the joint PDF is given by

$$p_{\gamma_{(1)}, \dots, \gamma_{(M)}}(x_1, \dots, x_M) = M! \binom{L}{M} [F(x_M)]^{L-M} \prod_{k=1}^M p(x_k) \tag{1}$$

where  $x_1 \geq \dots \geq x_M \geq 0$  and  $p(\cdot)$  and  $F(\cdot)$  correspond to the PDF and CDF of the SNR for a single channel reception (no-diversity case), respectively. By recognizing that the MGF of the combiner output SNR  $\phi_\gamma(\cdot)$  is the key to the unified analysis of many modulation/detection schemes over wireless channels, our immediate intention will be to derive the desired MGF first. Let  $\gamma = \gamma_{gsc} = \sum_{k=1}^M \gamma_{(k)}$  denote the hybrid combiner output SNR (see Fig. 1). Then, the MGF of  $\gamma_{gsc}$  may be computed as in (2), shown at the bottom of the next page [16]. The above multivariate integral (2) can be transformed into a univariate integral using identity (A.2), viz.

$$\phi_\gamma(s) = M \binom{L}{M} \int_0^\infty e^{-sx} p(x) [F(x)]^{L-M} [\phi(s, x)]^{M-1} dx \tag{3}$$

TABLE I  
PDF AND MARGINAL MGF OF SNR FOR A SINGLE DIVERSITY PATH IN DIFFERENT FADING CHANNEL MODELS

Channel Model	PDF $p(x)$ and marginal MGF $\phi(s, x) = \int_x^\infty e^{-sx} p(t) dt$ of SNR
Rayleigh	$p(x) = \frac{1}{\Omega} \exp(-x/\Omega), x \geq 0$ , where $\Omega = E[x]$ = average SNR/symbol/path $\phi(s, x) = \frac{\exp[-x(s+1/\Omega)]}{1+s\Omega}, s \geq 0$
Rician	$p(x) = \frac{1+K}{\Omega} \exp\left[-K - \frac{(1+K)x}{\Omega}\right] I_0\left[2\sqrt{\frac{K(K+1)x}{\Omega}}\right], x \geq 0$ , where $K \geq 0$ is the Rice factor $\phi(s, x) = \frac{1+K}{s\Omega+K+1} \exp\left[\frac{-sK\Omega}{s\Omega+K+1}\right] Q\left(\sqrt{\frac{2K(K+1)}{s\Omega+K+1}}, \sqrt{\frac{2(s\Omega+K+1)x}{\Omega}}\right), s \geq 0$ where $Q(\cdot, \cdot)$ denotes the first-order Marcum $Q$ -function
Nakagami- $m$	$p(x) = \frac{1}{\Gamma(m)} \left(\frac{m}{\Omega}\right)^m x^{m-1} \exp(-\frac{mx}{\Omega}), x \geq 0$ where $m \geq 0.5$ is the fading severity index $\phi(s, x) = \frac{1}{\Gamma(m)} \left(\frac{m}{m+s\Omega}\right)^m \Gamma(m, xs + xm/\Omega), s \geq 0$ where $\gamma(\cdot, \cdot)$ and $\Gamma(\cdot, \cdot)$ denote the incomplete Gamma function and its complement
Nakagami- $q$	$p(x) = \frac{1}{\Omega\sqrt{1-b^2}} \exp\left[\frac{-x}{(1-b^2)\Omega}\right] I_0\left[\frac{bx}{(1-b^2)\Omega}\right], x \geq 0$ , where $-1 \leq b = \frac{1-q^2}{1+q^2} \leq 1$ $\phi(s, x) = \frac{1}{\sqrt{(s\Omega+1)^2 - (s\Omega b)^2}} - \frac{\sqrt{1-b^2}}{s(1-b^2)\Omega+1} I_e\left[\frac{b}{s(1-b^2)\Omega+1}, \frac{s(1-b^2)\Omega x}{s(1-b^2)\Omega+1}\right], s \geq 0$ where $I_e[\cdot, \cdot]$ denotes the Rice's $I_e$ -function and $0 \leq q_k \leq \infty$ is the fading severity index

$$\begin{aligned} \phi_\gamma(s) &= \int_0^\infty \int_0^{x_1} \cdots \int_0^{x_{M-1}} e^{-s \sum_{k=1}^M x_k} p_{\gamma(1), \dots, \gamma(M)}(x_1, \dots, x_M) dx_M \cdots dx_2 dx_1 \\ &= M! \binom{L}{M} \int_0^\infty e^{-sx_M} p(x_M) [F(x_M)]^{L-M} \underbrace{\int_{x_M}^\infty e^{-sx_{M-1}} p(x_{M-1}) \cdots \int_{x_2}^\infty e^{-sx_1} p(x_1) dx_1 \cdots dx_{M-1}}_{(M-1)\text{-fold integral}} dx_M. \end{aligned}$$

where  $\phi(s, x) = \int_x^\infty e^{-st} p(t) dt$  denotes the marginal MGF of SNR of a single diversity branch, and  $F(x) = 1 - \phi(0, x)$ . If  $\phi(s, x)$  can be evaluated in closed form, then it is apparent from (3) that the computational complexity of  $\phi_\gamma(\cdot)$  involves only one-dimension integration [instead of an  $M$ -fold integration as in the case of (2)] because the integrand can be evaluated term by term for different values of  $x$ . The net result is a considerable reduction in computational complexity of  $\phi_\gamma(\cdot)$ , which is illustrated by (2). Table I summarizes both  $p(x)$  and  $\phi(s, x)$  needed in (3) for the different multipath fading environments.

For the purpose of numerical computations, it is much more desirable to rewrite (3) as

$$\begin{aligned} \phi_\gamma(s) &= M \binom{L}{M} \int_0^{\pi/2} e^{-s \tan \theta} p(\tan \theta) [1 - \phi(0, \tan \theta)]^{L-M} \\ &\quad \times [\phi(s, \tan \theta)]^{M-1} \sec^2 \theta d\theta \quad (4) \end{aligned}$$

since (4) has finite integration limits. Besides, (3) and/or (4) can be evaluated very efficiently using a Gauss-Chebyshev

quadrature (GCQ) method. From this viewpoint, (4) will yield a significant improvement over [14] in terms of computational complexity for the specific case of i.i.d. Nakagami- $m$  channels because the latter involves an  $M$ -dimensional GCQ sum, whereas in our case, we need to compute only a single (one-dimension) GCQ sum. Moreover, in Appendix B, we show that  $\phi_\gamma(\cdot)$ , which is defined in (3), may be evaluated in closed form when  $\gamma_1, \gamma_2, \dots, \gamma_L$  are i.i.d. exponential or gamma variates.

### B. PDF and CDF of GSC Output SNR

The PDF of GSC output SNR can be evaluated as [20]

$$p_r(x) \cong \frac{4}{T} \sum_{\substack{n=1 \\ n \text{ odd}}}^{\infty} \Re \left[ \phi_\gamma \left( \frac{-j2\pi n}{T} \right) \exp \left( \frac{-j2\pi n x}{T} \right) \right] \quad (5)$$

where  $j = \sqrt{-1}$ , and the coefficient  $T$  selected is sufficiently large, such that  $\Pr(x > T) \leq \epsilon$  and  $\epsilon$  can be set to a very small value. The above PDF may also be used for an ABER or ASER analysis of the coherent, differentially coherent, and noncoherent digital-modulation schemes in conjunction with the GSC( $M, L$ ) receiver.

$$\begin{aligned} \phi_\gamma(s) &= \int_0^\infty \int_0^{x_1} \cdots \int_0^{x_{M-1}} e^{-s \sum_{k=1}^M x_k} p_{\gamma(1), \dots, \gamma(M)}(x_1, \dots, x_M) dx_M \cdots dx_2 dx_1 \\ &= M! \binom{L}{M} \int_0^\infty e^{-sx_M} p(x_M) [F(x_M)]^{L-M} \underbrace{\int_{x_M}^\infty e^{-sx_{M-1}} p(x_{M-1}) \cdots \int_{x_2}^\infty e^{-sx_1} p(x_1) dx_1 \cdots dx_{M-1}}_{(M-1)\text{-fold integral}} dx_M. \quad (2) \end{aligned}$$

The knowledge of the CDF of  $\gamma_{\text{gsc}}$  is also of interest because the outage probability  $P_{\text{out}}$  of GSC diversity systems can be expressed in terms of this metric alone. Numerical computation based on [16, eq. (14)] indicates that the Fourier series converge slowly at low values of  $F_\gamma(x)$ ; we therefore exploit the Laplace inversion method suggested in [21] to compute for the CDF of  $\gamma_{\text{gsc}}$ , viz.

$$F_\gamma(x) \cong 2^{1-C} e^{A/2} \sum_{c=0}^C \binom{C}{c} \times \sum_{b=0}^{c+B} (-1)^b \alpha_b \Re \left[ \phi_\gamma \left( \frac{A + j2\pi b}{2x} \right) / (A + j2\pi b) \right] \quad (6)$$

where  $\alpha_0 = 0.5$ ,  $\alpha_b = 1$  for any  $b \geq 1$ , and the constants  $A$ ,  $B$ , and  $C$  are arbitrarily chosen to be 30, 18, and 24, respectively, which yield a good numerical accuracy for our purpose.

Since  $P_{\text{out}}$  is defined as the probability that the instantaneous symbol error rate of the system will exceed a specified value (say  $P_e^*$ ), (6) can be used to predict the efficacy of a GSC diversity receiver on the outage probability metric, viz.,  $P_{\text{out}} = F_\gamma(\gamma^*)$ , where  $\gamma^*$  is the threshold SNR. Given a digital-modulation scheme with a conditional error probability (CEP)  $P_s(\gamma)$ ,  $\gamma^*$  is obtained by solving  $P_s(\gamma^*) = P_e^*$ . For example, if  $P_e^* = 10^{-3}$  is specified,  $P_{\text{out}} = F(4.77)$  because  $\gamma^* = [\text{erfc}^{-1}(2 \times 10^{-3})]^2 = 4.77$  for a BPSK modulation scheme. Similarly, for QPSK or square four-QAM,  $P_{\text{out}} = F_\gamma(10.83)$ .

Fig. 2 depicts the CDF curves as a function of normalized mean SNR/symbol/branch  $\Omega/\gamma^*$  for the GSC( $M$ , 5) receiver in a Rician channel ( $K = 3$ ). Using these curves, it is possible to determine the mean SNR/symbol/branch to satisfy an outage requirement when a GSC( $M$ , 5) receiver is employed. For instance, if  $P_{\text{out}} = 10^{-2}$  is specified, then the mean SNR/symbol/branch requirement for a BPSK modulation may be estimated as  $\Omega = 4.77 (10^{-0.21}) = 4.69$  dB (interpolated from Fig. 2), assuming that  $M = 3$  and  $L = 5$ . If QPSK is used rather than BPSK, then  $\Omega = 10.83 (10^{-0.21}) = 8.25$  dB. Thus, to achieve the same outage probability, QPSK modulation requires approximately a 3.56-dB higher mean SNR/symbol/branch compared to BPSK for GSC(3, 5) at Rice factor  $K = 3$ . While higher order alphabets allow higher data transmission rates, the increased bandwidth efficiency is attained at the expense of increasing the mean SNR/symbol/branch requirement (to compensate for denser signaling constellation). It is also apparent from Fig. 2 that the relative diversity improvement diminishes with an increasing  $M$ .

### C. Mean Combined SNR

The mean combined SNR is another useful performance measure of diversity systems. Since the mean combined SNR  $\bar{\gamma}_{\text{gsc}}$  is the first moment (mean) of the RV  $\gamma_{\text{gsc}}$ , it can be determined by differentiating the MGF (3) with respect to  $s$  and then evaluating the derivative at  $s = 0$ . However, it is much

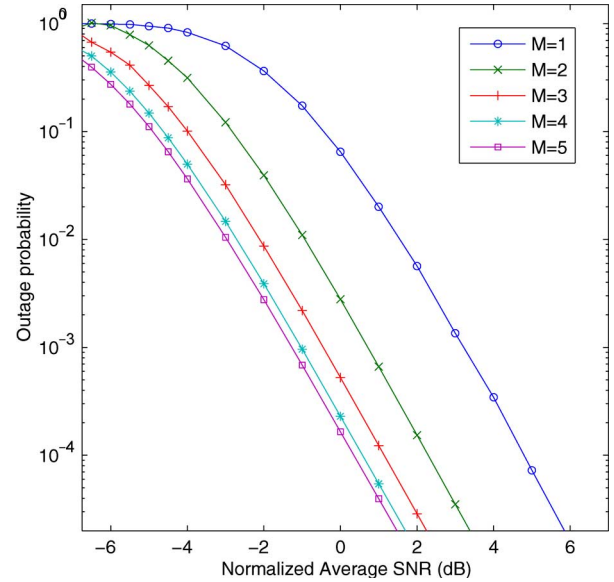


Fig. 2. Outage probability  $F_\gamma(\gamma^*)$  versus the normalized average SNR  $\Omega/\gamma^*$  for GSC( $M$ , 5) receiver in a Rician fading channel ( $K = 3$ ).

simpler to derive an expression for  $\bar{\gamma}_{\text{gsc}}$  by computing the sum of the expected value of the individual ordered SNRs as

$$\bar{\gamma}_{\text{gsc}} = \sum_{k=1}^M \bar{\gamma}_{(k)} \quad (7)$$

and by utilizing the density function of the  $k$ th strongest branch SNR  $\gamma_{(k)}$  from a population of  $L$  i.i.d. RVs  $\gamma_1, \gamma_2, \dots, \gamma_L$  given by [13]

$$p_{\gamma_{(k)}}(x) = k \binom{L}{k} [F(x)]^{L-k} [1 - F(x)]^{k-1} p(x). \quad (8)$$

Thus, we obtain

$$\bar{\gamma}_{\text{gsc}} = \sum_{k=1}^M k \binom{L}{k} \int_0^\infty x [F(x)]^{L-k} [1 - F(x)]^{k-1} p(x) dx \quad (9)$$

which may be computed efficiently via Gauss–Legendre quadrature method. It should be stressed that (9) holds for all values of  $M, L$  as well as for different fading environments. Higher order statistics (e.g., variance of GSC output SNR) can also be derived using a similar approach.

In Fig. 3, the normalized mean combined SNR at the GSC output  $\bar{\gamma}_{\text{gsc}}/\Omega$  is plotted as a function of diversity order  $L$  for different  $M$  values. For a fixed  $M$ , we observe that  $\bar{\gamma}_{\text{gsc}}/\Omega$  increases with an increasing diversity order  $L$ . The rate at which the normalized mean output SNR increases declines gradually as  $(L - M)$  increases, which is typical of the selection diversity systems. Also, for a fixed value of  $L$ ,  $\bar{\gamma}_{\text{gsc}}/\Omega$  increases with  $M$ , as expected.

Comparing the two subplots of Fig. 3, we note that the normalized mean combined SNR curve for a specified  $M$  and  $L$  becomes flatter as the channel experiences fewer deep fades (higher  $K$  values). This anomaly can be explained by

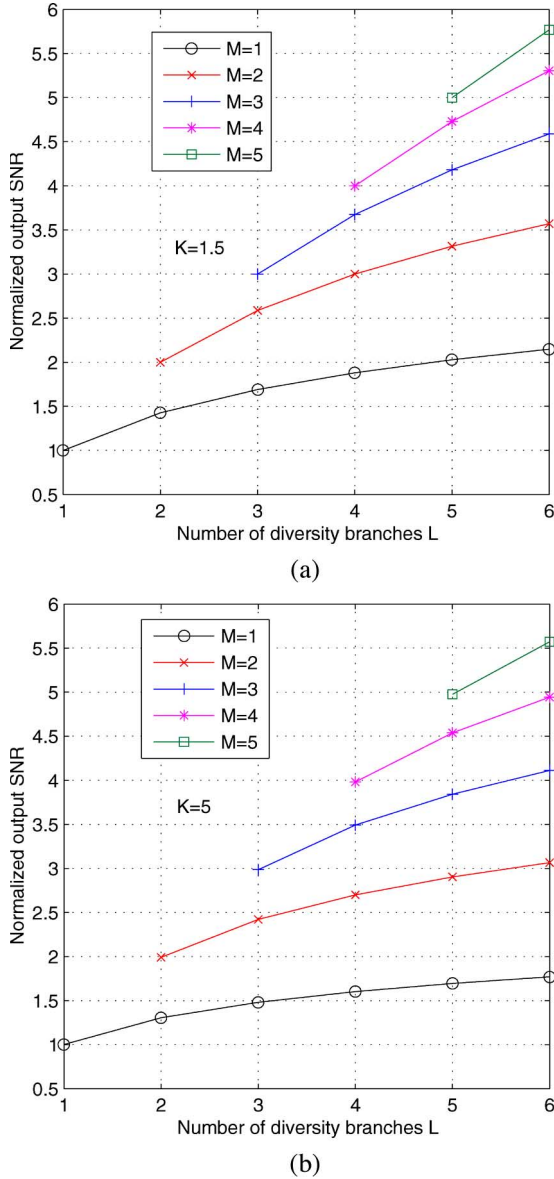


Fig. 3. Normalized mean GSC output SNR  $\bar{\gamma}_{\text{gsc}}/\Omega$  versus the total number of diversity branches  $L$  for various  $M$  values in a Rician channel. (a)  $K = 1.5$ . (b)  $K = 5$ .

considering the limiting case of an additive white Gaussian noise (AWGN) (nonfading) channel, in which the mean combined SNR is independent of the diversity order  $L$  and depends only on  $M$  (the number of paths combined at the receiver). Thus, as the channel condition improves, the statistical gain realized by ordering and choosing the strongest branch SNRs goes on decreasing, and the dominating factor is the total energy captured by combining additional diversity paths.

From Fig. 4, we observe that  $\bar{\gamma}_{\text{gsc}}/\Omega = 5$  for GSC(5, 5), and this value is independent of the fading severity index  $m$  of a Nakagami- $m$  channel. This trend is in agreement with the well-known result  $\bar{\gamma}_{\text{mrc}} = L\Omega$  for a maximal-ratio combining (MRC) receiver with  $L$  i.i.d. diversity branches. The dependence of  $\bar{\gamma}_{\text{gsc}}/\Omega$  on the fading parameter becomes more pronounced as  $M$  decreases. We also found that the normalized mean output SNR asymptotically approaches  $M$  as the fading index gets very large (i.e.,  $\lim_{m \rightarrow \infty} \bar{\gamma}_{\text{gsc}}/\Omega = M$ ).

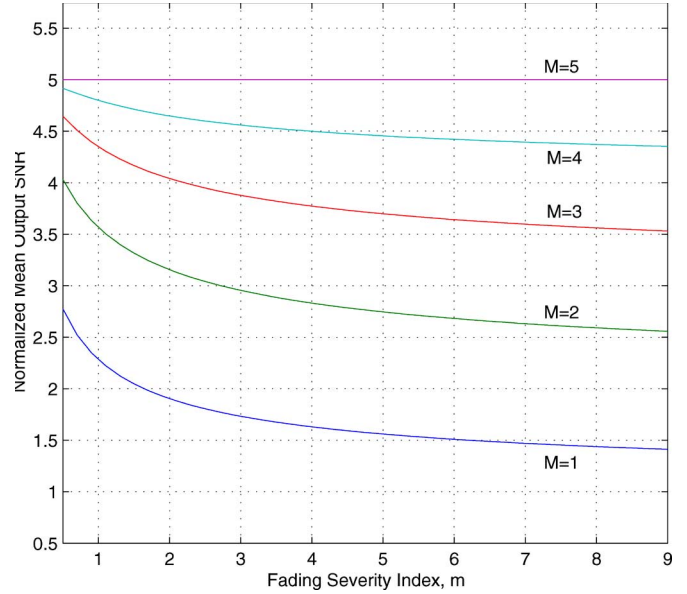


Fig. 4. Normalized mean output SNR of GSC( $M$ , 5) versus the fading severity index of Nakagami- $m$  channel for various selections of  $M$ .

### III. ASER ANALYSIS

In this section, we derive ASER expressions for a multitude of digital-modulation schemes in conjunction with the coherent and noncoherent GSC receiver structures with i.i.d. diversity paths using (4) or (5). If (4) is used, the final ASER expression will be in the form of a finite-range integral whose integrand is composed of only the MGF of the GSC output SNR  $\phi_\gamma(\cdot)$ . On the other hand, when (5) is used for the ASER computation, the resulting expression is a convergent infinite sum whose summand is composed of a product of  $\phi_\gamma(\cdot)$  and the Fourier transform (FT) of the CEP. Several examples are provided next to highlight the utility of the MGF and PDF of  $\gamma_{\text{gsc}}$  in the ASER analysis.

#### A. Coherent GSC Receiver

Using the MGF approach [8], [15], the ASER of  $M$ -ary PSK with the coherent GSC receiver is given by

$$\bar{P}_s = \frac{1}{\pi} \int_0^{\pi - \frac{\pi}{M_c}} \phi_\gamma \left( \frac{\sin^2(\pi/M_c)}{\sin^2 \theta} \right) d\theta \quad (10)$$

where  $M_c$  denotes the alphabet size of  $M$ -ary signal constellations, and  $\phi_\gamma(\cdot)$  is defined in (4).

Although the coherent GSC receiver is typically employed for the coherent modulation/detection schemes (i.e., channel estimates are required for the coherent diversity combining implementation), the analyses of the noncoherent modulation schemes with the coherent GSC receivers are also of interest because they provide a lower bound on the error rates with the noncoherent GSC receivers. This is particularly useful if the CEP for the multichannel quadratic receivers are not known or are in a complicated form. For instance, the ASER of  $M$ -ary

TABLE II  
MODULATION RELATED PARAMETERS FOR SEVERAL NONCOHERENT DIFFERENTIALLY COHERENT COMMUNICATION SYSTEMS

Modulation	$a$	$b$	$\eta$
DPSK	0	$\sqrt{2}$	1
BFSK	0	1	1
$\pi/4$ -DQPSK	$\sqrt{2 - \sqrt{2}}$	$\sqrt{2 + \sqrt{2}}$	1

differential phase-shift keying (DPSK) with the coherent GSC receiver is given by

$$\bar{P}_s = \frac{1}{\pi} \int_0^{\pi - \frac{\pi}{M_c}} \phi_\gamma \left[ \frac{\sin^2(\pi/M_c)}{1 + \cos(\pi/M_c) \cos \theta} \right] d\theta. \quad (11)$$

For the special case of binary DPSK ( $M_c = 2$ ), (11) simplifies to  $\bar{P}_b = \phi_\gamma(1)/2$ .

Using the procedure above, it is also possible to write down ASER formulas for other modulation schemes. They are omitted here for brevity.

**B. Noncoherent GSC Receiver**

Since square-law detection (also known as postdetection equal-gain combining) circumvents the need to cophase and weigh the diversity branches, the multichannel quadratic receiver has a simple implementation and is suitable for use in noncoherent and differentially coherent communication systems [2].

The ABER performance of DPSK, BFSK, and  $\pi/4$ -DQPSK in conjunction with a noncoherent GSC( $M, L$ ) receiver may be computed using [28]

$$\bar{P}_b = \frac{1}{(1 + \eta)^{2M-1} 2\pi} \int_0^{2\pi} \frac{g(\theta)}{1 - 2\beta \cos \theta + \beta^2} \times \phi_\gamma \left[ \frac{b^2}{2} (1 - 2\beta \cos \theta + \beta^2) \right] d\theta \quad (12)$$

where  $0^+ < \beta = a/b < 1$

$$g(\theta) = \sum_{k=0}^{2M-1} \binom{2M-1}{k} \beta^{k+1-M} \eta^k \times \{ \cos [(k - M + 1)\theta] - \beta \cos [(k - M)\theta] \} \quad (13)$$

and the values for  $a, b,$  and  $\eta$  for the three different modulation schemes are summarized in Table II.

Note that, as  $\beta \rightarrow 0$ , (12) assumes an indeterminate form, but its limit converge smoothly to the exact ABER. Thus, the ABER of DPSK and BFSK can be computed using (12) with good accuracy by setting  $a = 10^{-3}$  instead of zero. Alternatively, one may utilize (5) to average over the CEP of multichannel communication to yield the following an infinite series formula for the ABER:

$$\bar{P}_b \cong \frac{4}{T} \sum_{\substack{n=1 \\ n \text{ odd}}}^{\infty} \Re \left[ \phi_\gamma \left( \frac{-j2\pi n}{T} \right) G_\gamma \left( \frac{2\pi n}{T} \right) \right] \quad (14)$$

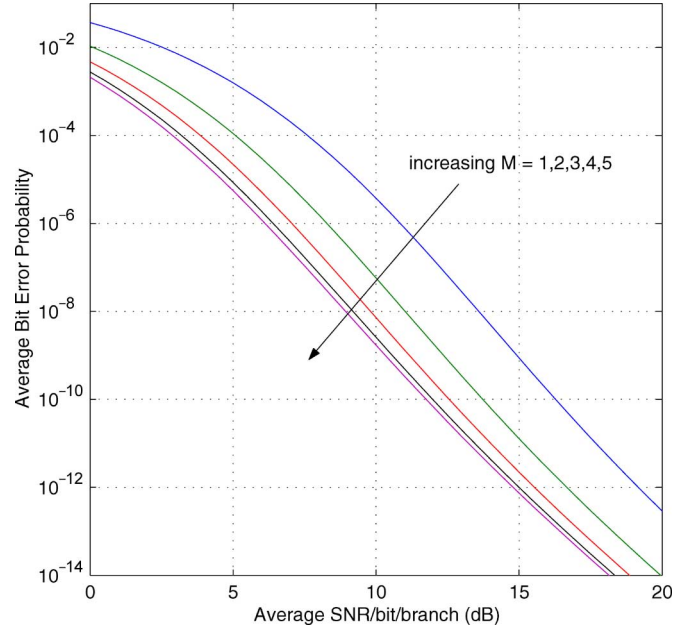


Fig. 5. ABER performance of the BPSK with GSC( $M, 5$ ) receiver in a Rician fading channel ( $K = 3.5$ ).

where  $G_\gamma(\omega) = \text{FT}[P_b(\gamma)] = \int_0^\infty P_b(\gamma) e^{-j\omega\gamma} d\gamma$ . For instance,  $G_\gamma(\omega)$  for  $M$ -ary orthogonal FSK with the noncoherent GSC( $M, L$ ) receiver is given by

$$G_\gamma(\omega) = \frac{M_c}{2(M_c - 1)} \sum_{n=1}^{M_c-1} \binom{M_c - 1}{n} \sum_{k=0}^{n(M-1)} \beta(k, n, M) \times \sum_{i=0}^k \binom{M + k - 1}{k - i} \frac{(-1)^{n+1} k!}{(1 + n)^{M+k+i}} \times \left[ \left( \frac{n}{1 + n} \right)^2 + \omega^2 \right]^{-(i+1)/2} \times \exp \left[ -j(i + 1) \tan^{-1} \left( \frac{\omega}{n} (n + 1) \right) \right] \quad (15)$$

by utilizing the closed-form CEP formula derived in [22]. This approach may be extended to the other digital-modulation schemes. Details can be found in [23].

**C. Numerical Examples**

Fig. 5 shows the ABER performance for BPSK modulation with a receiver in a Rician fading environment (Rice factor  $K = 3.5$ ). All the performance curves are upper and lower bounded by GSC(1, 5) and GSC(5, 5), which correspond to the selection diversity combining (SDC) and the MRC schemes, respectively. Moreover, the performance curve for GSC( $M, 5$ ) quickly move toward the MRC case as  $M$  is increased gradually (the gap between the curves gets closer). For example, at the ABER of  $10^{-5}$ , the diversity gains for GSC(2, 5) and GSC(3, 5) are approximately 2.6 and 3.8 dB, respectively, with respect to the SDC receiver. It is also observed that these gains remain almost constant particularly at the low error rates.

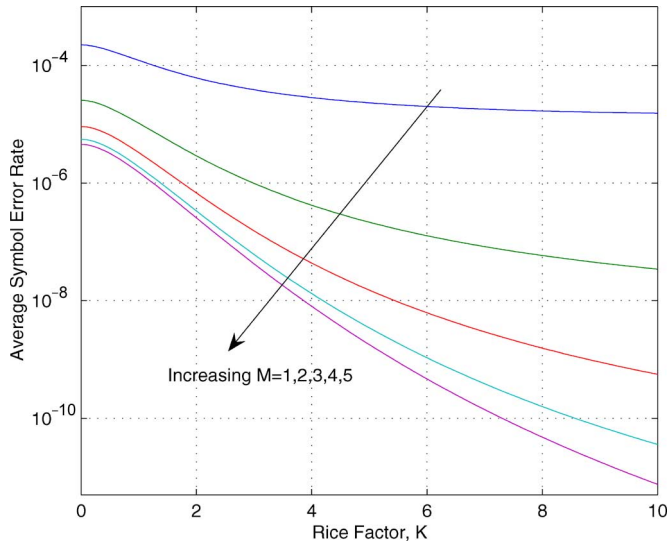


Fig. 6. ASER of the QPSK as a function of the Rice factor  $K$  for GSC( $M$ , 5) receiver and average SNR/symbol/branch  $\Omega = 12$  dB.

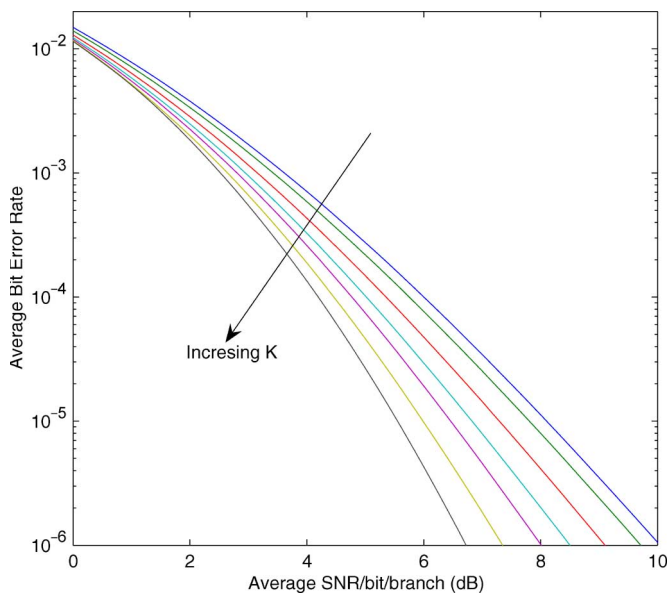


Fig. 7. ABER of the DPSK with a coherent GSC(3, 6) receiver for the different Rice factors  $K \in \{0, 0.5, 1, 1.5, 2, 3, 5\}$ .

In Figs. 6 and 7, we illustrate the effect of fade distributions on the error probability performance of QPSK and DPSK modulation schemes in conjunction with a coherent GSC receiver. Even though the ASER decreases as the channel condition improves, the slope of the curves (i.e., rate of decay) in Fig. 6 is a function of the number of diversity paths combined at the receiver. The diversity improvement observed from Fig. 6 is attributed to the following two factors: 1) statistical gain realized by ordering and choosing the strongest branch SNRs and 2) total energy captured by combining additional diversity paths. The former depends on both the fading parameter  $K$  and the difference between  $L$  and  $M$ , while the latter is dictated only by the number of combined diversity paths  $M$ .

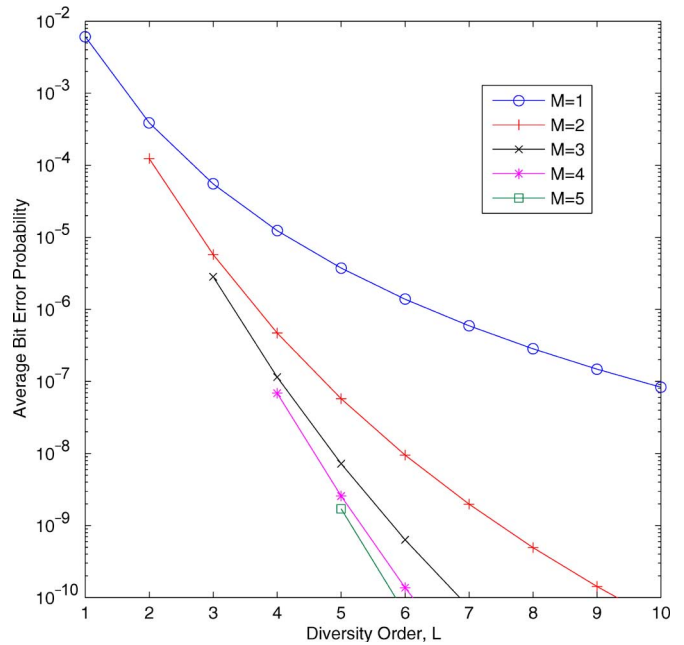


Fig. 8. ABER of the BPSK versus the diversity order  $L$  for different  $M$  in a Rician channel with  $K = 3.5$  and mean SNR/bit/branch  $\Omega = 10$  dB.

Looking at the trends in Fig. 6, we may conclude that factor 1) has a stronger influence in severe fading conditions while factor 2) to be predominant in a less severely faded environments [i.e., the ABER curve for GSC(1, 5) becomes almost flat for  $K > 6$ ]. While GSC( $M$ , 5) with a moderate  $M$  value (say  $M = 3$ ) yields a comparable performance with that of MRC in severely faded wireless channels (e.g.,  $K = 0$ ), the discrepancy between them gets larger as the Rice factor increases (see Fig. 6). Thus, it is highly desirable to combine more diversity paths to improve the overall receiver performance when strong specular components are available. It is apparent from Fig. 7 that the effect of fade distribution on ABER performance becomes more pronounced as  $\Omega$  increases.

Fig. 8 depicts the ABER variation for BPSK modulation as a function of diversity order  $L$ . It is evident that increasing  $L$  also translates into a considerable improvement in the receiver performance. However, the relative improvement with higher order diversities declines because the probability of deep fades decreases with an increasing  $M$  and/or  $L$ . Fig. 8 may also be used to investigate the benefits/tradeoff between various combinations of  $L$  and  $M$  in a receiver design. For example, the ABER performance obtained with selection combining having  $L = 10$  may be realized using diversity orders as low as GSC(2, 5) or even GSC(3, 4), given that the mean SNR/bit/branch  $\Omega = 10$  dB.

The error performance of DQPSK in conjunction with the coherent and noncoherent GSC( $M$ , 5) receiver structures in a Rician fading environment ( $K = 2.5$ ) are illustrated in Fig. 9. The ABER of DQPSK with a coherent GSC receiver may be computed as [25]

$$\bar{P}_b = \frac{1}{2\pi} \int_0^\pi \phi_\gamma \left( \frac{2}{2 - \sqrt{2} \cos \theta} \right) d\theta \quad (16)$$

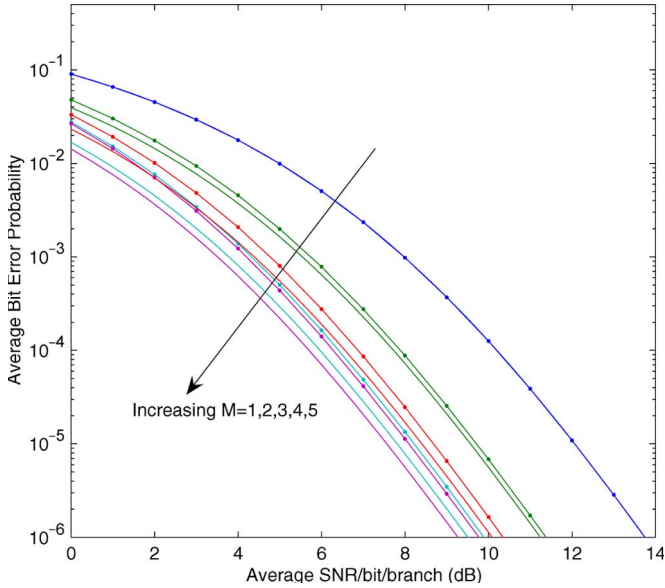


Fig. 9. ABER performance of  $\pi/4$ -DQPSK with coherent (solid lines) and noncoherent (circle marked lines) GSC( $M, 5$ ) receiver structures in a Rician fading environment ( $K = 2.5$ ).

and the ABER with a noncoherent GSC receiver is given by (12).

For the special case of selection diversity, both predetection combining and postdetection combining perform identically. The difference between the coherent and noncoherent GSC gets larger as  $M$  increases. For the small and moderate  $M$  values, however, the noncoherent GSC is attractive, owing to its simple implementation and because it yields comparable performance with that of the coherent GSC receiver. We also observe that, for a fixed  $M$  value, the ABER performance with a noncoherent GSC asymptotically approaches the ABER performance with a coherent GSC receiver (i.e., the gap between the curves gets smaller as the mean SNR/bit/branch  $\Omega$  increases).

#### IV. CONCLUSION

This paper investigates the performance of both the coherent and noncoherent GSC( $M, L$ ) receivers with i.i.d. diversity paths in Rician fading, which heretofore had resisted solution in a simple form. Unified expressions for computing the MGF, PDF, and CDF of a GSC output SNR in a myriad of fading environments are also derived. Several new closed-form formulas for the MGF of GSC output SNR in i.i.d. Nakagami- $m$  fading are also derived. The MGF and PDF of  $\gamma_{\text{gsc}}$  are used to facilitate ASER analysis for different modulation/detection schemes, while the outage probability performance is predicted from the CDF expression. A simple formula for computing the average combined SNR is also presented.

#### APPENDIX A

In this Appendix, we show that the  $(M - 1)$ -fold nested integral in (2) can be replaced by a closed-form formula (in terms of the marginal MGF alone) without imposing any restrictions on the fade distribution.

Define  $I(s, x_M)$  as

$$I(s, x_M) = \int_{x_M}^{\infty} e^{-sx_{M-1}} p(x_{M-1}) \cdots \int_{x_2}^{\infty} e^{-sx_1} p(x_1) dx_1 \cdots dx_{M-1}. \quad (\text{A.1})$$

We will prove (using the principles of mathematical induction) that

$$I(s, x_M) = \frac{[\phi(s, x_M)]^{M-1}}{(M - 1)!}, \quad M \geq 2 \quad (\text{A.2})$$

where  $\phi(s, x) = \int_x^{\infty} e^{-st} p(t) dt$  denotes the marginal MGF of SNR of a single diversity branch. This also implies that  $(d/dx)\phi(s, x) = -e^{-sx} p(x)$ .

For  $M = 2$ , we have

$$I(s, x_2) = \int_{x_2}^{\infty} e^{-sx_1} p(x_1) dx_1 = \phi(s, x_2) \quad (\text{A.3})$$

implying that (A.2) holds for  $M = 2$ . Assume that (A.2) holds for  $M = N - 1$ . This implies

$$I(s, x_{N-1}) = \frac{[\phi(s, x_{N-1})]^{N-2}}{(N - 2)!}. \quad (\text{A.4})$$

Using the definition (A.1) and the assumption (A.4), we can write  $I(s, x_N)$  as

$$I(s, x_N) = \int_{x_N}^{\infty} e^{-sx_{N-1}} p(x_{N-1}) I(s, x_{N-1}) dx_{N-1} = \int_{x_N}^{\infty} e^{-sx_{N-1}} p(x_{N-1}) \frac{[\phi(s, x_{N-1})]^{N-2}}{(N - 2)!} dx_{N-1}. \quad (\text{A.5})$$

Applying integration by parts on (A.5), we get

$$I(s, x_N) = -\phi(s, x_{N-1}) \frac{[\phi(s, x_{N-1})]^{N-2}}{(N - 2)!} \Big|_{x_N}^{\infty} - \int_{x_N}^{\infty} \frac{[\phi(s, x_{N-1})]^{N-3}}{(N - 3)!} e^{-sx_{N-1}} \times p(x_{N-1}) \phi(s, x_{N-1}) dx_{N-1}. \quad (\text{A.6})$$

Noting that  $\phi(s, \infty) = 0$ , we can simplify (A.6) and obtain

$$I(s, x_N) = \frac{[\phi(s, x_N)]^{N-1}}{(N - 2)!} - (N - 2)I(s, x_N) \quad (\text{A.7})$$

implying that (A.2) holds for  $M = N$ . Therefore, by mathematical induction, (A.2) holds for all  $M \geq 2$ . Substituting (A.2)

into (2), we obtain a univariate integral expression for the MGF of GSC output SNR:

$$\phi_\gamma(s) = M \binom{L}{M} \int_0^\infty e^{-sx_M} p(x_M) [F(x_M)]^{L-M} \times [\phi(s, x_M)]^{M-1} dx_M \quad (\text{A.8})$$

which is valid for all combinations of  $L$  and  $M \leq L$  as well as for different fading environments. For the special case of  $M = L$ , the resulting  $M$ -fold integral for  $\phi_\gamma(\cdot)$  given by (2) can also be evaluated using identity (A.2) as

$$\phi_\gamma(s) = [\phi(s, 0)]^L = [\phi(s)]^L \quad (\text{A.9})$$

as expected [note:  $\phi(s)$  corresponds to the MGF of SNR in the no-diversity case].

It should be emphasized that (A.8) collapses into a single integral expression with finite integration limits [see (4)], while the fading signal amplitudes follow either the Rician or the Nakagami- $m$  (real  $m \geq 0.5$ ) or the Nakagami- $q$  distribution. This is attributed to the availability of closed-form solutions for the marginal MGF  $\phi(s, x)$  in the above cases (see Table I). Moreover, if  $\gamma_1, \gamma_2, \dots, \gamma_L$  are i.i.d. exponential or gamma variates, (A.8) can also be evaluated in closed form as described in Appendix B.

## APPENDIX B

Regardless of the branch of science or engineering, theoreticians have always been enamored with the notion of expressing their results in the form of closed-form formulas. Motivated by this, we attempted to show that (3) can be evaluated in closed form if  $\gamma_1, \gamma_2, \dots, \gamma_L$  are i.i.d. exponential or gamma variates. These developments are illustrated next.

In a Rayleigh fading environment, the individual path SNRs  $\gamma_k (k \in \{1, 2, \dots, L\})$  will follow an exponential distribution. Substituting the appropriate PDF and marginal MGF from Table I into (3), we obtain (after simplification)

$$\phi_\gamma(s) = \frac{M \binom{L}{M}}{(1+s\Omega)^{M-1}} \sum_{k=0}^{L-M} \frac{(-1)^k \binom{L-M}{k}}{[M(1+s\Omega) + k]}. \quad (\text{B.1})$$

We may also utilize the well-known relation  $\gamma_{(k)} = \sum_{r=k}^L (\gamma_r/r)$  from the spacing property [26] of ordered exponential RVs to derive  $\phi_\gamma(\cdot)$ . Since  $\gamma_{\text{gsc}}$  can be expressed as a linear combination of independent standard unordered exponential RVs with an appropriate weighting

$$\begin{aligned} \gamma_{\text{gsc}} &= \sum_{k=1}^M \gamma_{k:L} = \sum_{k=1}^M \sum_{r=k}^L \frac{\gamma_r}{r} \\ &= \gamma_1 + \gamma_2 + \dots + \gamma_{M-1} + \sum_{r=M}^L \frac{M\gamma_r}{r} \end{aligned} \quad (\text{B.2})$$

and noting that the MGF of each  $\gamma_r$  is given by  $1/(1+s\Omega)$ , we immediately obtain the following equation by observation:

$$\phi_\gamma(s) = \frac{1}{(1+s\Omega)^{M-1}} \prod_{r=M}^L \frac{1}{(1+s\Omega M/r)}. \quad (\text{B.3})$$

Incidentally, this result is identical to those given in [7] and [8]. Our derivation, however, is much more direct and simple. It is further pointed out that the virtual-path transformation method introduced in [7] is identical to the spacing method [26]; and this result has been known in the mathematics literature for decades. Now, let us turn our attention to the derivation of closed-form formula for  $\phi_\gamma(\cdot)$  in Nakagami- $m$  channels (real  $m \geq 1/2$ ). By substituting the PDF and marginal MGF in (3), we obtain

$$\begin{aligned} \phi_\gamma(s) &= \frac{M(m/\Omega)^m}{[\Gamma(m)]^{L-M+1}} \binom{L}{M} \left( \frac{m}{m+s\Omega} \right)^{m(M-1)} \\ &\times \sum_{k=0}^{M-1} \binom{M-1}{k} \left[ \frac{-1}{\Gamma(m)} \right]^k \\ &\times \int_0^\infty x^{m-1} e^{-x(s+m/\Omega)} [\gamma(m, xm/\Omega)]^{L-M} \\ &\times [\gamma(m, x(s+m/\Omega))]^k dx. \end{aligned} \quad (\text{B.4})$$

where  $\gamma(a, x) = \Gamma(a) - \Gamma(a, x)$  is the incomplete gamma function. Therefore, we need to solve the generic integral

$$I_n = \int_0^\infty x^{\nu-1} e^{-cx} \prod_{k=1}^n \gamma(a_k, b_k x) dx, \quad n \geq 0. \quad (\text{B.5})$$

The special cases  $I_0$  and  $I_1$  have been treated in [24, eq. (3.381.4)] and [24, eq. (6.455.2)], respectively. Using these results, it is possible to evaluate (B.4) in closed form for  $L = 2$  and  $M \in \{1, 2\}$ . Similar simplifications appear to be difficult when  $L \geq 2$ , except for the limiting case  $M = L$ . Therefore, we first utilize identity  $\gamma(a, x) = x^a e^{-x} {}_1F_1(1; 1+a; x)/a$  [24, eq. (8.351.2)] to rewrite the integrand of (B.5) as a product of Kummer  ${}_1F_1(\cdot; \cdot; \cdot)$  functions and then exploit [27, eq. (C.1)] to get a new integral identity involving a product of incomplete gamma functions in the following:

$$\begin{aligned} I_n &= \left[ \prod_{k=1}^n \frac{(b_k)^{a_k}}{a_k} \right] \int_0^\infty x^{\nu-1 + \sum_{k=1}^n a_k - x(c + \sum_{k=1}^n b_k)} \\ &\times \prod_{k=1}^n {}_1F_1(1; 1+a_k; b_k x) dx \\ &= \left[ \prod_{k=1}^n \frac{(b_k)^{a_k}}{a_k} \right] \frac{\Gamma(\nu + \alpha)}{(c + \beta)^{\nu + \alpha}} F_A \\ &\times \left( \underbrace{\nu + \alpha; 1, \dots, 1}_{n \text{ terms}}; 1 + a_1, \dots, 1 \right. \\ &\left. + a_n; \frac{b_1}{c + \beta}, \dots, \frac{b_n}{c + \beta} \right) \end{aligned} \quad (\text{B.6})$$

where  $\alpha = \sum_{k=1}^n a_k$ ,  $\beta = \sum_{k=1}^n b_k$ , and the Lauricella's hypergeometric function with several variables  $F_A(\cdot; \cdot; \cdot; \cdot)$  is defined as [24, Eq. (9.19)]

$$F_A(\alpha; \beta_1, \dots, \beta_n; \gamma_1, \dots, \gamma_n; z_1, \dots, z_n) = \sum_{m_1=0}^{\infty} \dots \sum_{m_n=0}^{\infty} \frac{(\alpha)_{m_1+\dots+m_n} (\beta_1)_{m_1}, \dots, (\beta_n)_{m_n}}{(\gamma_1)_{m_1}, \dots, (\gamma_n)_{m_n} m_1! \dots m_n!} \times z_1^{m_1}, \dots, z_n^{m_n} \quad (\text{B.7})$$

and the notation  $(a)_n = \Gamma(a+n)/\Gamma(a)$  denotes the Pochhammer symbol. The identity (B.6) holds if the conditions  $a_k > -1$ ,  $\nu + \alpha > 0$ , and  $c > 0$  are satisfied. Thus, using (B.6) and (B.4), we obtain the following:

$$\begin{aligned} \phi_\gamma(s) &= \frac{M m^{(L-M)(m-1)+m}}{[\Gamma(m)]^{L-M+1}} \binom{L}{M} \left( \frac{m}{m+s\Omega} \right)^{m(M-1)} \\ &\times \sum_{k=0}^{M-1} \binom{M-1}{k} \left[ \frac{-1}{\Gamma(m)} \right]^k \\ &\times \frac{\Gamma[m(L-M+k+1)] (s\Omega+m)^{mk}}{m^k [(s\Omega+m)(k+1) + (L-M)m]^{m(L-M+k+1)}} \\ &\times F_A \left( \underbrace{m(L-M+k+1)}_{L-M+k}; \underbrace{1, \dots, 1}_{L-M+k}; \right. \\ &\quad \left. \underbrace{1+m, \dots, 1+m}_{L-M+k}; \underbrace{X, \dots, X}_{L-M}; \underbrace{Y, \dots, Y}_{k \text{ terms}} \right) \end{aligned} \quad (\text{B.8})$$

where  $X = m/[(s\Omega+m)(k+1) + (L-M)m]$  and  $Y = (s\Omega+m)/[(s\Omega+m)(k+1) + (L-M)m]$ . To the best of our knowledge, the above development is new.

This development is also interesting in view of the general belief that a closed-form formula for MGF of GSC( $M, L$ ) in Nakagami- $m$  fading with arbitrary real  $m$  is ordinarily unobtainable [12]. It should be noted, however, that the elegance of the above closed-form formula is overshadowed by the complexity of the numerical computation for  $L \geq 4$  compared to (3).

For the special case of  $[L = 2, M = 1]$ , (B.8) reduces into

$$\begin{aligned} \phi_\gamma(s) &= \frac{2\Gamma(2m)}{m [\Gamma(m)]^2} \left( \frac{m}{s\Omega + 2m} \right)^{2m} \\ &\times {}_2F_1 \left( 2m, 1; 1+m; \frac{m}{2m+s\Omega} \right) \end{aligned} \quad (\text{B.9})$$

where  ${}_2F_1(a; b; c; z) = \sum_{n=0}^{\infty} [(a)_n (b)_n z^n] / [(c)_n n!]$ ,  $|z| < 1$  is the Gauss hypergeometric function.

Similarly, for  $[L = 2, M = 2]$ , (B.8) simplifies into

$$\phi_\gamma(s) = \left( \frac{m}{s\Omega + m} \right)^{2m} \quad (\text{B.10})$$

once we recognize that  ${}_2F_1[a; b; (a+b+1)/2; 1/2] = \sqrt{\pi} \Gamma[(a+b+1)/2] / \{\Gamma[(a+1)/2] \Gamma[(b+1)/2]\}$  and  $\Gamma(m+1/2) = 2^{1-2m} \sqrt{\pi} \Gamma(2m) / \Gamma(m)$ .

If  $m$  assumes a positive integer value, then computational complexity of  $\phi_\gamma(\cdot)$  depicted in (B.8) can be improved considerably. In this case, (3) can be restated very concisely as

$$\begin{aligned} \phi_\gamma(s) &= \frac{M}{\Gamma(m)} \binom{L}{M} \sum_{k=0}^{L-M} (-1)^k \binom{L-M}{k} \\ &\times \sum_{n=0}^{(M-1)(m-1)} \beta(n, M-1, m) \sum_{z=0}^{k(m-1)} \beta(z, k, m) \\ &\times \frac{\Gamma(z+n+m) m^{mM+z}}{(m+s\Omega)^{m(M-1)-n} [sM\Omega + m(M+k)]^{z+n+m}} \end{aligned} \quad (\text{B.11})$$

once we recognize  $\phi(s, x) = [m/(m+s\Omega)]^m \exp[-x(s+m/\Omega)] \sum_{k=0}^{M-1} (1/k!) [x(s+m/\Omega)]^k$ . The multinomial coefficients  $\beta(\cdot, \cdot, \cdot)$  in (B.11) may be computed as

$$\beta(k, n, d) = \sum_{i=k-d+1}^k \frac{\beta(i, n-1, d)}{(k-i)!} I_{[0, (n-1)(d-1)]}(i) \quad (\text{B.12})$$

where  $I_{[a,b]}(i) = \begin{cases} 1, & a \leq i \leq b \\ 0, & \text{otherwise} \end{cases}$ ,  $\beta(0, 0, d) = \beta(0, k, d) = 1$ ,  $\beta(k, 1, d) = (1/k!)$ , and  $\beta(1, n, d) = n$ .

Equation (B.11) is much more efficient than the recursive formula for the MGF derived in [15]. It is also interesting to note that (B.11) can be used to derive closed-form formulas for a variety of digital-modulation schemes in conjunction with GSC( $M, L$ ) receiver over Nakagami- $m$  channels (positive integer fading severity index). They are omitted here for brevity.

#### ACKNOWLEDGMENT

The authors would like to thank the anonymous reviewers for their valuable comments and suggestions, which enhanced the quality of this paper.

#### REFERENCES

- [1] N. Kong, T. Eng, and L. B. Milstein, "A selection combining scheme for rake receivers," in *Proc. IEEE ICUPC*, 1995, pp. 426-430.
- [2] T. Eng, N. Kong, and L. B. Milstein, "Comparison of diversity combining techniques for Rayleigh-fading channels," *IEEE Trans. Commun.*, vol. 44, no. 9, pp. 1117-1129, Sep. 1996.
- [3] K. J. Kim, S. Y. Kwon, E. K. Hong, and K. C. Whang, "Comments on comparison of diversity combining techniques for Rayleigh-fading channels," *IEEE Trans. Commun.*, vol. 46, no. 9, pp. 1109-1110, Sep. 1998.
- [4] T. Eng, N. Kong, and L. Milstein, "Correction to "Comparison of diversity combining techniques for Rayleigh-fading channels,"" *IEEE Trans. Commun.*, vol. 46, no. 9, p. 1111, Sep. 1998.
- [5] N. Kong and L. Milstein, "Average SNR of a generalized diversity selection combining scheme," *IEEE Trans. Commun.*, vol. 3, no. 3, pp. 57-59, Mar. 1999.
- [6] N. Kong and L. B. Milstein, "SNR of generalized diversity selection combining with nonidentical Rayleigh fading statistics," *IEEE Trans. Commun.*, vol. 48, no. 8, pp. 1266-1271, Aug. 2000.
- [7] M. Win and J. Winters, "Analysis of hybrid selection/maximal-ratio combining in Rayleigh fading," *IEEE Trans. Commun.*, vol. 47, no. 12, pp. 1773-1776, Dec. 1999.

- [8] M.-S. Alouini and M. K. Simon, "An MGF-based performance analysis of generalized selection combining over Rayleigh fading channels," *IEEE Trans. Commun.*, vol. 48, no. 3, pp. 401–415, Mar. 2000.
- [9] A. Annamalai and C. Tellambura, "The effects of Gaussian weighting errors in hybrid SC/MRC receivers," in *Proc. IEEE Wireless Commun. and Netw. Conf.*, Sep. 2000, pp. 211–215.
- [10] R. Wong, A. Annamalai, and V. Bhargava, "Evaluation of predetection diversity techniques for RAKE receivers," in *Proc. IEEE PACRIM Commun., Comput., Signal Process.*, Victoria, BC, Canada, 1997, vol. 1, pp. 227–230.
- [11] M.-S. Alouini and M. Simon, "Performance of coherent receivers with hybrid SC/MRC over Nakagami- $m$  fading channels," *IEEE Trans. Veh. Technol.*, vol. 48, no. 4, pp. 1155–1164, Jul. 1999.
- [12] —, "Application of the Dirichlet transformation to the performance evaluation of generalized selection combining over Nakagami- $m$  fading channels," *J. Commun. Netw.*, vol. 1, no. 1, pp. 5–13, Mar. 1999.
- [13] A. Annamalai and C. Tellambura, "Error rates of hybrid SC/MRC diversity systems on Nakagami- $m$  channels," in *Proc. IEEE Wireless Commun. and Netw. Conf.*, Sep. 2000, pp. 227–231.
- [14] Y. Ma and C. C. Chai, "Unified error probability analysis for generalized selection combining in Nakagami fading channels," *IEEE J. Sel. Areas Commun.*, vol. 18, no. 11, pp. 2198–2210, Nov. 2000.
- [15] A. Annamalai and C. Tellambura, "Performance evaluation of generalized selection diversity systems over Nakagami- $m$  fading channels," *Wirel. Commun. Mob. Comput. (UK)*, vol. 3, no. 1, pp. 41–56, Feb. 2003.
- [16] —, "A new approach to performance evaluation of generalized selection diversity receivers in wireless channels," in *Proc. IEEE VTC*, Atlantic City, NJ, 2001, vol. 4, pp. 2309–2313.
- [17] S. Stein, "Fading channel issues in system engineering," *IEEE J. Sel. Areas Commun.*, vol. SAC-5, no. 2, pp. 68–89, Feb. 1987.
- [18] M. Nakagami, "The  $m$ -distribution, a general formula of intensity distribution of rapid fading," in *Statistical Methods in Radio Wave Propagation*, W. G. Hoffman, Ed. Oxford, U.K.: Pergamon, 1960.
- [19] A. Papoulis, *Probability, Random Variables, and Stochastic Processes*, 3rd ed. New York: McGraw-Hill, 1991.
- [20] N. C. Beaulieu, "An infinite series for the computation of the complementary probability distribution function of a sum of independent random variables and its application to the sum of Rayleigh random variables," *IEEE Trans. Commun.*, vol. 38, no. 9, pp. 1463–1474, Sep. 1990.
- [21] J. Abate and W. Whitt, "Numerical inversion of Laplace transforms of probability distribution," *ORSA J. Comput.*, vol. 7, no. 1, pp. 36–43, 1995.
- [22] A. Annamalai and C. Tellambura, "A moment-generating function (MGF) derivative-based unified analysis of incoherent diversity reception of  $M$ -ary orthogonal signals over independent and correlated fading channels," *Int. J. Wirel. Inf. Netw. (USA)*, vol. 10, no. 1, pp. 41–56, Jan. 2003.
- [23] A. Annamalai, C. Tellambura, and V. Bhargava, "A general method for calculating error probabilities over fading channels," in *Proc. IEEE ICC*, 2000, pp. 36–40.
- [24] I. S. Gradshteyn and I. M. Ryzhik, *Table of Integrals, Series, and Products*, 5th ed. New York: Academic, 1994.
- [25] A. Annamalai and C. Tellambura, "Error rates for Nakagami- $m$  fading multichannel reception of binary and  $M$ -ary signals," *IEEE Trans. Commun.*, vol. 49, no. 1, pp. 58–68, Jan. 2001.
- [26] P. V. Suhatme, "Tests of significance for samples of the  $\chi^2$  population with two degree of freedom," *Ann. Eugen.*, vol. 8, pp. 52–56, 1937.
- [27] A. Annamalai, C. Tellambura, and V. Bhargava, "Equal-gain diversity receiver performance in wireless channels," *IEEE Trans. Commun.*, vol. 48, no. 10, pp. 1732–1745, Oct. 2000.
- [28] A. Annamalai, G. Deora, and C. Tellambura, "Unified error probability analysis for generalized selection diversity in Rician fading channels," in *Proc. IEEE VTC*, Birmingham, AL, 2002, vol. 4, pp. 2042–2046.

**A. Annamalai** (S'90–M'99) received the B.Eng. degree (with the highest distinction) from University of Science of Malaysia, Minden, P. Pinang, Malaysia, in 1993 and the M.A.Sc. and Ph.D. degrees from University of Victoria, Victoria, BC, Canada, in 1997, and 1999, respectively, all in electrical and computer engineering.

From May 1993 to April 1995, he was with Motorola's Land Mobile Products Sector as a Research and Development Engineer. Since December 1999, he has been working as a Faculty Member with the Bradley Department of Electrical and Computer Engineering, Virginia Tech., Blacksburg. His current research interests are in adaptive radios, cooperative mesh networks, ultrawideband communications, smart antennas, and wireless communication theory.

Dr. Annamalai has received several awards for excellence in research, including the 2001 IEEE Leon Kirchmayer Prize Paper Award for his work on diversity systems, the 2000 NSERC Doctoral Prize, and the 2000 CAGS/UMI Distinguished Dissertation Award in the Natural Sciences, Medicine, and Engineering. He has served with the editorial boards of four IEEE journals as an Associate Editor and with organizing committees of IEEE conferences in wireless communications, including the 56th IEEE Vehicular Technology Conference in the capacity of Technical Program Chair.

**Gautam Deora** received the B.Eng. degree in electronics (with distinction) from Bombay University, Bombay, India, in 2000 and the M.S.E.E. degree from Virginia Tech., Arlington, VA, in 2002.

From June 2000 to May 2001, he was a Graduate Research Assistant with the Mobile and Portable Radio Research Group (MPRG) at Virginia Tech., where he was involved in developing low-complexity receiver structures for CDMA, ultrawideband (UWB), and satellite digital radio systems. Between July 2002 and May 2003, he was as a Research Engineer with the Center for Remote Sensing Inc., working on GPS position location and real time kinematic algorithms. Since August 2003, he has been working with the Applied Technology Group at Tata Infotech, working on WiFi-based solutions, radio frequency identification (RFID), and related wireless technologies.

**C. Tellambura** (M'97–SM'02) received the B.Sc. degree (with first-class honors) from University of Moratuwa, Moratuwa, Sri Lanka, in 1986, the M.Sc. degree in electronics from University of London, London, U.K., in 1988, and the Ph.D. degree in electrical engineering from University of Victoria, Victoria, BC, Canada, in 1993.

He was a Postdoctoral Research Fellow with the University of Victoria from 1993 to 1994 and the University of Bradford, Bradford, U. K., from 1995 to 1996. He was with the Monash University, Melbourne, Australia, from 1997 to 2002. Presently, he is a Professor with the Department of Electrical and Computer Engineering, University of Alberta, Edmonton, AB, Canada. His research interests include coding, communication theory, modulation, equalization, and wireless communications.

Prof. Tellambura is an Associate Editor for both the IEEE TRANSACTIONS ON COMMUNICATIONS and the IEEE TRANSACTIONS ON WIRELESS COMMUNICATIONS. He was the Chair of the Communication Theory Symposium in Globecom'05, St. Louis, MO.